

# Electronic-Insulating Coating of CaCO<sub>3</sub> on TiO<sub>2</sub> Electrode in Dye-Sensitized Solar Cells: Improvement of Electron Lifetime and Efficiency

Zhong-Sheng Wang,\* Masatoshi Yanagida, Kazuhiro Sayama, and Hideki Sugihara\*

National Institute of Advanced Industrial Science and Technology (AIST),  
1-1-1, Higashi, Tsukuba, Ibaraki 305-8565, Japan

Received February 7, 2006

Electronic-insulating coating of CaCO<sub>3</sub> on nanocrystalline TiO<sub>2</sub> electrode for dye-sensitized solar cells was found to increase both short-circuit photocurrent ( $J_{sc}$ ) and open-circuit photovoltage ( $V_{oc}$ ) remarkably. The significant increase in  $J_{sc}$  is mainly attributed to the remarkably increased dye adsorption resulting from the more basic surface of CaCO<sub>3</sub> than TiO<sub>2</sub>, while the increase in  $V_{oc}$  originates from suppression of charge recombination owing to the surface covering of TiO<sub>2</sub> with an insulating coating of CaCO<sub>3</sub>, revealed by intensity-modulated photovoltage spectroscopy. A 15  $\mu\text{m}$  TiO<sub>2</sub> (23 nm) nanocrystalline electrode coated with 1 wt % CaCO<sub>3</sub>, sensitized with N719, produced power conversion efficiency of 10.2%, where N719 is *cis*-di(thiocyanato)-bis(2,2'-bipyridyl-4,4'-dicarboxylate) ruthenium(II), using an antireflective film on the cell surface.

## Introduction

Dye-sensitized solar cells (DSSCs) offer the hope of fabricating photovoltaic devices with high efficiency at low cost.<sup>1</sup> *cis*-Di(thiocyanato)-bis(2,2'-bipyridyl-4,4'-dicarboxylate)ruthenium(II), the so-called N719, has shown outstanding performance with an efficiency of greater than 10%.<sup>2,3</sup> However, a challenge to optimize N719 toward efficiency still remains since its theoretical efficiency is about 14%.<sup>4</sup>

Nanocrystalline TiO<sub>2</sub> particles are not perfect in terms of solar cell efficiency in that the charge recombination between injected electrons and electron acceptors (e.g., I<sub>3</sub><sup>-</sup> ions) in the electrolyte is unavoidable to diminish both photovoltage and photocurrent, thus limiting the device efficiency.<sup>5,6</sup> To improve device efficiency, one effective approach is to grow a thin coating layer of another oxide on the TiO<sub>2</sub> surface.<sup>7–11</sup> This overlayer, which has a higher conduction band edge than TiO<sub>2</sub>, is reported to be effective to retard charge recombination and hence improve device efficiency.<sup>12</sup>

As TiO<sub>2</sub> nanocrystalline films can be coated with various materials, the coated TiO<sub>2</sub> photoelectrode should have photovoltaic performance related to the nature and amount of the coating materials. While there have been considerable efforts of coating TiO<sub>2</sub> with large band-gap semiconducting metal oxides,<sup>7–12</sup> little attention has been paid to electronic-insulating materials<sup>13</sup> as the coating layer to retard charge recombination in DSSCs. CaCO<sub>3</sub> is an electronic insulator. Therefore, coating TiO<sub>2</sub> with CaCO<sub>3</sub> may be effective to physically separate the injected electrons and electron acceptors (i.e., I<sub>3</sub><sup>-</sup> ions) and hence retard charge recombination in DSSCs. In addition, CaCO<sub>3</sub> is more basic than TiO<sub>2</sub>, favoring higher dye adsorption and thus higher light-harvesting efficiency (LHE). On the basis of these considerations, we chose CaCO<sub>3</sub> as being representative of electronic-insulating materials to study the coating effect on the electron lifetime during electron transport in the mesoporous TiO<sub>2</sub> film and device performance.

## Experimental Section

TiO<sub>2</sub> nanoparticles (23 nm) and scattering particles (100 nm) were prepared with the method reported previously.<sup>14</sup> One-layer transparent films (6  $\mu\text{m}$ ) and three-layer TiO<sub>2</sub> films (5  $\mu\text{m}$  for each layer), which were employed in this work, were fabricated using various pastes with a screen-printing method. Three kinds of TiO<sub>2</sub> pastes, N consisting of 23 nm particles, M' consisting of a mixture of 23 and 100 nm particles with a molar ratio of 8:2, and M consisting of a mixture of 23 and 100 nm particles with a molar ratio of 6:4, were prepared using ethyl cellulose as a binder and

\* To whom correspondence should be addressed. Phone: +81-29-861-4643. Fax: +81-29-861-6771. E-mail: zs.wang@aist.go.jp.

- (1) O'Regan, B.; Grätzel, M. *Nature* **1991**, *353*, 737.
- (2) Nazeerudin, M. K.; Kay, A.; Rodicio, I.; Humphry-Baker, R.; Müller, E.; Liska, P.; Vlachopoulos, N.; Grätzel, M. *J. Am. Chem. Soc.* **1993**, *115*, 6382.
- (3) Grätzel, M. *J. Photochem. Photobiol. A* **2004**, *164*, 3.
- (4) Frank, A. J.; Kopidakis, N.; Lagemaat, J. V. D. *Coord. Chem. Rev.* **2004**, *248*, 1165.
- (5) Haque, S. A.; Tachibana, Y.; Willis, R. L.; Moser, J. E.; Grätzel, M.; Klug, D. R.; Durrant, J. R. *J. Phys. Chem. B* **2000**, *104*, 538.
- (6) Gregg, B. A.; Pichot, F.; Ferrere, S.; Fields, C. L. *J. Phys. Chem. B* **2001**, *105*, 1422.
- (7) Jung, H. S.; Lee, J.-K.; Nastasi, M.; Lee, S.-W.; Kim, J.-Y.; Park, J.-S.; Hong, K. S.; Shin, H. *Langmuir* **2005**, *21*, 10332.
- (8) Zaban, A.; Chen, S. G.; Chappel, S.; Gregg, B. A. *Chem. Commun.* **2000**, 2231.
- (9) Kay, A.; Grätzel, M. *Chem. Mater.* **2002**, *14*, 2930.
- (10) Tennakone, K.; Kumara, G. R. R. A.; Kottegoda, I. R. M.; Perera, V. P. S. *Chem. Commun.* **1999**, 15.
- (11) Wang, Z.-S.; Huang, C.-H.; Huang, Y.-Y.; Hou, Y.-J.; Xie, P.-H.; Zhang, B.-W.; Cheng, H.-M. *Chem. Mater.* **2001**, *13*, 678.

- (12) Palomares, E.; Clifford, J. N.; Haque, S. A.; Lutz, T.; Durrant, J. R. *J. Am. Chem. Soc.* **2003**, *125*, 475.
- (13) Okada, N.; Karuppuchamy, S.; Kurihara, M. *Chem. Lett.* **2005**, *34*, 16.
- (14) Wang, Z. S.; Kawauchi, H.; Kashima, T.; Arakawa, H. *Coord. Chem. Rev.* **2004**, *248*, 1381.

$\alpha$ -terpineol as a solvent. One-layer transparent films were fabricated using paste N, while three-layer NM'M films were fabricated by printing paste N, M', and M subsequently onto glass substrate coated with transparent conductive oxide (TCO, F-doped SnO<sub>2</sub>, sheet resistance 8–10  $\Omega/\square$ , Nippon Sheet Glass, Japan). The films were calcined at 525 °C for 2 h after each deposition. After dipping in 0.1 M calcium acetate aqueous solution for 20 min at room temperature, the films were washed with water and dried with N<sub>2</sub> flow followed by firing at 525 °C for 30 min. The amount of CaCO<sub>3</sub> coating was controlled by simply repeating the dipping/sintering cycle for desired times. Both the coated and uncoated films, when they were at about 150 °C, were dipped in a N719 (Solaronix SA) solution (0.3 mM in 1/1(v/v) acetonitrile/*tert*-butyl alcohol) for 24 h.

The sandwich-type solar cell was assembled by placing a platinum-coated TCO glass (counter electrode) on the N719 dye-sensitized photoelectrode (working electrode). The two electrodes were separated by a hot-melt Surlyn spacer (30  $\mu\text{m}$  thick) and sealed by heating the Surlyn frame at 105 °C.<sup>15</sup> The redox electrolyte was introduced into the space of interelectrodes through the two holes predrilled on the back of the counter electrode. The two holes were sealed using a Surlyn film on which a glass slide was pressed under 105 °C.<sup>15</sup> The redox electrolyte used was 0.1 M LiI, 0.05 M I<sub>2</sub>, 0.6 M 1,2-dimethyl-3-*n*-propylimidazolium iodide, and 0.5 M 4-*tert*-butylpyridine in dried acetonitrile. The current–voltage characteristics of the cells were measured with a dc voltage current source/monitor (Advantest, R6246). An AM1.5 solar simulator (Yamashita Denso Co., YSS-150A with a 1000-W Xe lamp and an AM1.5 filter) was employed as the light source. The incident light intensity was calibrated with a standard Si solar cell equipped with a KG-5 filter, which was produced by Japan Quality Assurance Organization. Photocurrent action spectra, incident photon-to-electron conversion efficiency (IPCE) plotted as a function of excitation wavelength, were recorded on a CEP-99W system (Bunkoh-Keiki Co., Ltd.). It is worth noting that black painting was applied to the bare TCO part around the dye-coated film during the measurement; otherwise,  $J_{\text{sc}}$  would be overestimated by 10–15% because some photons impinging on the bare TCO glass can penetrate to the N719 dye-loaded film through reflection and refraction by the glass texture.<sup>14,16</sup> The apparent cell size was 0.5 cm  $\times$  0.5 cm, and the active area was precisely measured with a Nikon digital camera controlled by a computer using an objective micrometer as a reference.

The UV–vis absorption spectra of the dye-loaded transparent film were recorded on a Shimadzu UV-3101PC UV–Vis–NIR spectrophotometer. The attenuated total reflection Fourier transform infrared (ATR-FTIR) spectra were measured with a Perkin-Elmer Spectrum One spectrophotometer. The X-ray photoelectron spectrum (XPS) was collected at a take-off angle of 75° using a ULVAC Physical Electronics XPS-1800 spectrometer with the Al K $\alpha$  line (1486.6 eV). The intensity-modulated photovoltage spectroscopy (IMVS) at open circuit was performed on an impedance/gain-phase analyzer (Solartron SI 1260) under modulated illumination from a green diode laser (Samba, 532 nm, 50 mW, Cobolt Co.) and constant white light bias from a Xe lamp (Ushio, UXL-500D-O). The laser light was modulated with an Acousto-Optics modulator (Isomet Co., 1205C-1). The illumination of laser light with the white light bias was attenuated with appropriate neutral density filters to obtain various light intensities.

(15) Wang, Z.-S.; Sayama, K.; Sugihara, H. *J. Phys. Chem. B* **2005**, *109*, 22449.

(16) Wang, Z.-S.; Yamaguchi, T.; Sugihara, H.; Arakawa, H. *Langmuir* **2005**, *21*, 4272.

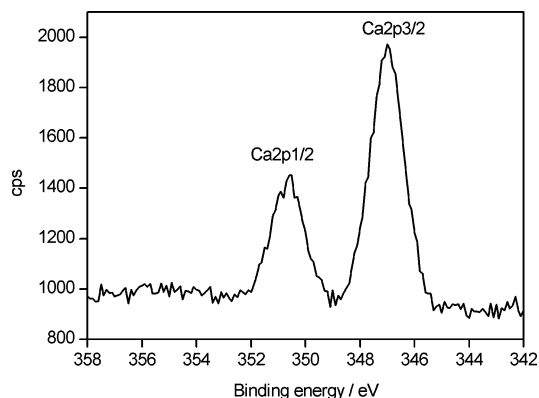
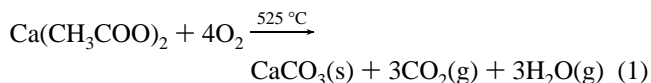


**Figure 1.** High-resolution XPS of Ca2p1/2 and 2p3/2 for CaCO<sub>3</sub>-coated transparent TiO<sub>2</sub> film (6  $\mu\text{m}$ ).

## Results and Discussion

Transparent TiO<sub>2</sub> films were used to carry out the characterizations. When a TiO<sub>2</sub> film was dipped in 0.1 M calcium acetate aqueous solution, Ca<sup>2+</sup> ions could be adsorbed specifically onto the TiO<sub>2</sub> surface through exchange with protons at the oxide/water interface.<sup>17</sup> A homogeneous layer of adsorbed cations with acetate is expected under the experimental conditions,<sup>9</sup> which is then converted into a CaCO<sub>3</sub> coating by firing at 525 °C.<sup>18</sup>



Formation of CaCO<sub>3</sub> overlayer on the TiO<sub>2</sub> surface was detected by XPS measurement. Figure 1 shows the XPS for the CaCO<sub>3</sub>-coated TiO<sub>2</sub> film. Peaks assignable to Ca2p3/2 and Ca2p1/2 were detected at 347.0 and 350.6 eV, respectively,<sup>19</sup> which agrees with the binding energies of Ca in CaCO<sub>3</sub> reported in the literature.<sup>19</sup> The molar ratio of Ca to Ti, determined through XPS quantification, was 0.8%. The amount of CaCO<sub>3</sub> formed on the TiO<sub>2</sub> surface is therefore deduced to be 10 mg per gram of TiO<sub>2</sub>, corresponding to 1 wt % CaCO<sub>3</sub>. The 2 and 3 wt % CaCO<sub>3</sub> coatings could be obtained by repeating the dipping/sintering cycle for 2 and 3 times, respectively.

To further confirm formation of calcium carbonate, ATR-FTIR spectra were measured for both CaCO<sub>3</sub>-coated and uncoated TiO<sub>2</sub> bare films (Figure 2). The peak at 1645 cm<sup>-1</sup> appearing in the spectra for both films is attributable to the bending mode of O–H groups in the adsorbed water. The IR spectrum of the untreated TiO<sub>2</sub> film is featureless except the peak for adsorbed water as seen in Figure 2. In contrast to untreated TiO<sub>2</sub>, two strong peaks at 1500 and 1393 cm<sup>-1</sup>, assignable to the asymmetric and symmetric O–C–O stretching vibrations, appear in the spectrum of the coated film, strongly supporting formation of carbonate.<sup>20</sup> Since

(17) Jang, H. M.; Fuerstenau, D. W. *Colloids Surf.* **1986**, *21*, 235.

(18) Thermogravimetric analysis indicated that calcium acetate was converted to calcium carbonate at the experimental conditions and stable up to 650 °C until decomposition.

(19) Moulder, J. F.; Stickle, W. F.; Sobol, P. E.; Bomben, K. D. *Handbook of X-ray Photoelectron Spectroscopy*; Physical Electronics, Inc.: Eden Prairie, MN, 1995.

(20) Villalobos, M.; Leckie, J. O. *J. Colloid Interface Sci.* **2001**, *235*, 15.

(21) Nazeerudin, M. K.; Splivallo, R.; Liska, P.; Comte, P.; Grätzel, M. *Chem. Commun.* **2003**, 1456.

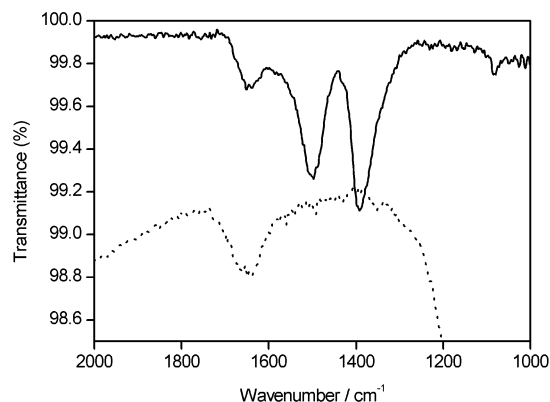


**Figure 2.** ATR-FTIR spectra for CaCO<sub>3</sub>-coated (solid line) and uncoated (dotted line) TiO<sub>2</sub> film (6 μm).

there is only one peak around 1393 cm<sup>-1</sup> for the free CO<sub>3</sub><sup>2-</sup> species, observation of two vibration peaks at 1500 and 1393 cm<sup>-1</sup> in the coated TiO<sub>2</sub> indicates formation of coordination bonds between the CO<sub>3</sub><sup>2-</sup> moiety and a surface Ti(IV).<sup>20</sup>

Since the binding mode of N719 to the TiO<sub>2</sub> surface may influence dye adsorption and thus photovoltaic performance, we compared the FTIR spectra (see Figure S1 in Supporting Information) for dye-loaded-coated and uncoated TiO<sub>2</sub>. FTIR data show that N719 anchors to the TiO<sub>2</sub> surface using the two carboxylic acid groups with bidentate coordination mode<sup>21</sup> because no peak for COOH at ~1720 cm<sup>-1</sup> is observed in N719-loaded TiO<sub>2</sub>.<sup>21</sup> N719-loaded TiO<sub>2</sub>/CaCO<sub>3</sub> gave a very similar FTIR spectrum to that for the untreated film, indicating that the CaCO<sub>3</sub> coating did not affect the binding mode of N719 to the TiO<sub>2</sub> surface. In addition, Brunauer-Emmett-Teller (BET) analysis showed that the BET surface area of TiO<sub>2</sub> powder taken from the film was not influenced noticeably by the coating of CaCO<sub>3</sub>, with a BET surface area of 59 ± 1 m<sup>2</sup>/g for both uncoated and coated films.

The isoelectric point of CaCO<sub>3</sub> (pH 8.3) is higher than that of anatase TiO<sub>2</sub> (pH 6.2),<sup>22</sup> indicating that the surface of the CaCO<sub>3</sub> coating is more basic than TiO<sub>2</sub>. The higher basicity of the CaCO<sub>3</sub>-coated surface favors dye attachment through its carboxylic acid groups.<sup>9,12</sup> Therefore, an increase in dye adsorption upon CaCO<sub>3</sub> coating is expected. Figure 3 shows the UV-vis absorption spectra for dye-loaded transparent film with and without CaCO<sub>3</sub> overlayer. As expected, the metal-to-ligand charge-transfer (MLCT) absorption peaks<sup>2</sup> significantly increased upon CaCO<sub>3</sub> coating on the TiO<sub>2</sub> surface. The absorbance of the lowest energy MLCT band increased from 0.413 to 0.517, corresponding to an increase in surface concentration<sup>2</sup> from 2.91 × 10<sup>-8</sup> to 3.64 × 10<sup>-8</sup> mol cm<sup>-2</sup> by 25%. This result was confirmed by UV-vis spectrophotometric determination of the dye solution obtained by desorbing the N719 dye on TiO<sub>2</sub> film into a 0.1 M NaOH solution.<sup>14</sup> N719 cannot cover the TiO<sub>2</sub> surface fully due to the intermolecular electrostatic repulsion. The presence of CaCO<sub>3</sub> strengthens the dye attachment to the TiO<sub>2</sub> surface due to the basicity of CaCO<sub>3</sub>, thus increasing the dye coverage. Considering that the incident light was absorbed approximately twice by the dye in solar cells with

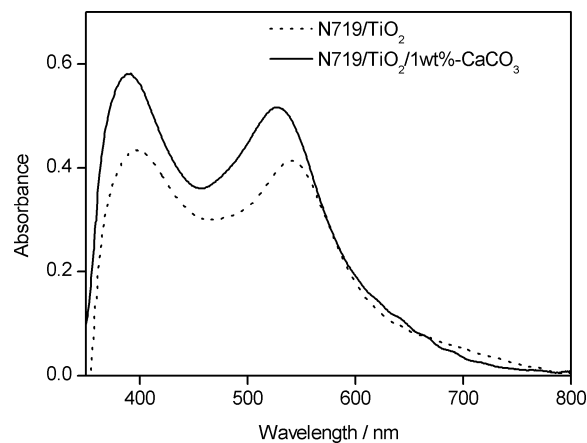


**Figure 3.** UV-vis absorption spectra for N719-loaded TiO<sub>2</sub> (6 μm) with and without CaCO<sub>3</sub> coating.

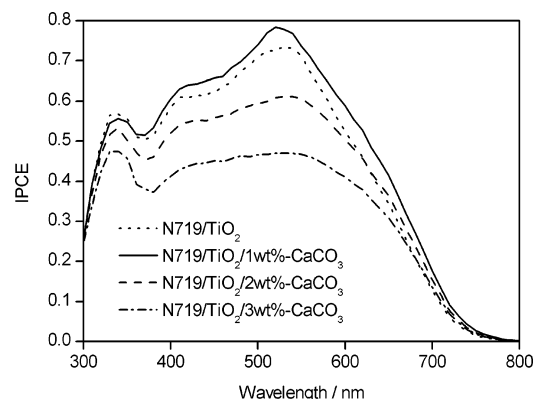


**Figure 4.** IPCE action spectra for solar cells with and without CaCO<sub>3</sub> coating; 6 μm transparent TiO<sub>2</sub> films were used.

a Pt mirror,<sup>2</sup> we calculated the LHE, to the first approximation, using  $LHE = 1 - 10^{-2A}$ , where  $A$  is the absorbance of dye-loaded TiO<sub>2</sub> (Figure 3). The LHEs at around 530 nm were estimated to be 85.1% and 90.8% for uncoated and CaCO<sub>3</sub>-coated TiO<sub>2</sub> films, respectively.

In addition, the two MLCT peaks were blue shifted from 540 to 528 nm and from 396 to 388 nm, respectively, upon CaCO<sub>3</sub> coating on the TiO<sub>2</sub> surface. The blue shift is attributed to the increased surface basicity due to CaCO<sub>3</sub> covering. It was reported that N719 showed almost same MLCT band positions in solution and on the TiO<sub>2</sub> surface.<sup>21</sup> Upon adsorption on TiO<sub>2</sub>, the carboxyl groups bind to Ti<sup>4+</sup> accompanied by proton release. The Lewis acid Ti<sup>4+</sup> or proton behaves as an electron-withdrawing moiety, lowering the energy of the π\* orbital and thus leading to similar MLCT band positions.<sup>21</sup> However, upon coating TiO<sub>2</sub> with CaCO<sub>3</sub>, the basicity of CaCO<sub>3</sub> raises the energy of the π\* orbital, resulting in blue shifts of MLCT bands.

The increased dye amount on the TiO<sub>2</sub> surface is anticipated to improve IPCE, which is defined as the number of electrons generated by light in the external circuit divided by the number of incident photons. Figure 4 shows the IPCE action spectra for solar cells with and without CaCO<sub>3</sub> layer in which the dependence of IPCE on the amount of CaCO<sub>3</sub> coating is also present. A 1 wt % coating was found to be optimal in terms of IPCE generation. The IPCEs between 360 and 750 nm are increased remarkably as a result of increased dye adsorption. The maximum IPCE was increased



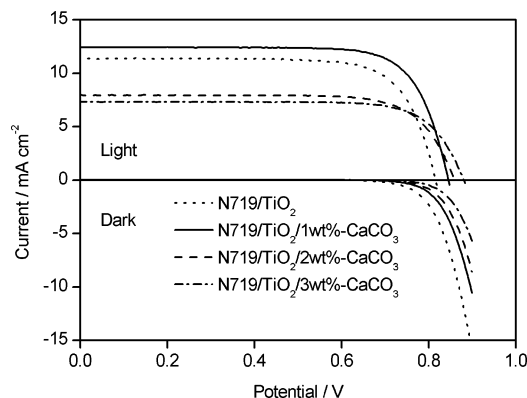


**Figure 5.**  $I$ - $V$  curves for the solar cells (same as those in Figure 4) under  $100 \text{ mW cm}^{-2}$  simulated AM1.5 light and in the dark.

from 73.4% to 78.4% by 6.8%, in good agreement with the increase in LHE of 6.7%. However, further increasing the coating amount resulted in decreased IPCE values despite the increased dye adsorption. The decrease in IPCE with increasing CaCO<sub>3</sub> coating amount might result from the decreased electron injection yield as reported in the literature.<sup>12</sup> Electron transfer from the excited dye to the conduction band of underlying TiO<sub>2</sub> occurred by tunneling through the insulating layer.<sup>9</sup> According to Figure 4, electron injection in the coated solar cell is as efficient as that in the uncoated one when the coating amount is  $\leq 1$  wt % but less efficient than the uncoated one when the coating amount is  $\geq 2$  wt %.

The peak at 340 nm observed in the action spectra is mainly attributed to direct excitation of TiO<sub>2</sub> under UV light.<sup>23</sup> We also observed a peak at this position for a solar cell with a bare TiO<sub>2</sub> film (i.e., without dye). IPCE at this position decreased gradually due to the covering of CaCO<sub>3</sub> in both the dye-loaded cell (Figure 4) and bare TiO<sub>2</sub> cell (not shown), indicating that covering of CaCO<sub>3</sub> prohibits band-gap excitation of TiO<sub>2</sub> under UV light, which may be favorable for long-term stability in the presence of UV light.<sup>9</sup>

Figure 5 shows the  $I$ - $V$  curves for the same cells used in Figure 4 under  $100 \text{ mW cm}^{-2}$  AM1.5 light and in the dark. The uncoated cell produced an overall efficiency of 6.9% ( $J_{\text{sc}} = 11.38 \text{ mA cm}^{-2}$ ,  $V_{\text{oc}} = 0.816 \text{ V}$ , FF = 0.741). Upon 1 wt % CaCO<sub>3</sub> coating on the TiO<sub>2</sub> surface, the overall efficiency was improved to 7.9% ( $J_{\text{sc}} = 12.41 \text{ mA cm}^{-2}$ ,  $V_{\text{oc}} = 0.845 \text{ V}$ , FF = 0.758). The increased  $J_{\text{sc}}$  resulted from the increased dye amount, consistent with the IPCE result. In addition to the significant increase in  $J_{\text{sc}}$ , enhancement of  $V_{\text{oc}}$  was also observed, which is attributed to the increased electron lifetime and reduced dark current as discussed later. Upon increasing the coating amount further,  $V_{\text{oc}}$  was further increased but  $J_{\text{sc}}$  decreased gradually, consistent with the IPCE result (Figure 4), leading to decreased overall efficiency of 5.0% for 2 wt % coating and 4.9% for 3 wt % coating. Again, it is verified from the  $I$ - $V$  data that the coating layer does not diminish electron injection when the coating amount is  $\leq 1$  wt % but prohibits electron injection when the coating amount is  $\geq 2$  wt %.

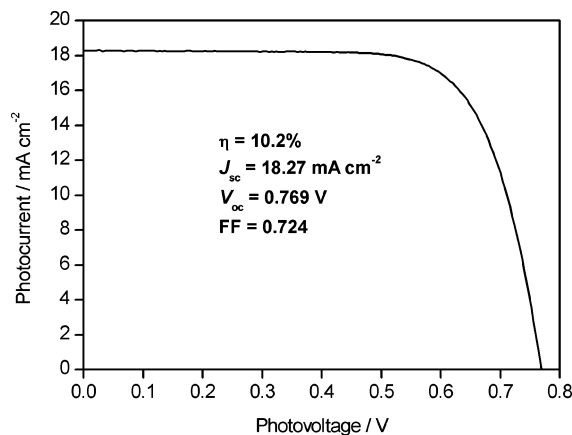


**Figure 6.**  $I$ - $V$  curve for dye-sensitized 1 wt % CaCO<sub>3</sub>-coated TiO<sub>2</sub> (NM'M) under  $100 \text{ mW cm}^{-2}$  simulated AM1.5 light using an antireflective film placed on the cell surface.

$I$ - $V$  curves in the dark (Figure 5) show that the dark current was reduced gradually with increasing CaCO<sub>3</sub> coating amount on the TiO<sub>2</sub> surface, indicating charge recombination between injected electrons and I<sub>3</sub><sup>-</sup> ions being retarded by the insulating layer. The reduction of dark current upon CaCO<sub>3</sub> coating on the TiO<sub>2</sub> surface accounts partly for the increased  $V_{\text{oc}}$  upon CaCO<sub>3</sub> coating.<sup>2</sup>

When scattering particles are incorporated into the matrix of transparent nanoparticles, device efficiency can be improved significantly through enhancing LHE by light scattering.<sup>2,14</sup> A 1 wt % CaCO<sub>3</sub> coating was still found to be effective to improve the efficiency of the high-efficiency cell (NM'M). The untreated NM'M film produced a power conversion efficiency from 8.26% to 8.64% for 10 parallel cells, averaging at 8.50% with a standard deviation of 0.16%. The 1 wt % CaCO<sub>3</sub>-coated NM'M film yielded a power conversion efficiency from 9.15% to 9.63% for 10 parallel samples, averaging at 9.40% with a standard deviation of 0.18%. Like the case of low-efficiency cells, the improvement of high-efficiency cells is also attributed to the increase in both  $J_{\text{sc}}$  and  $V_{\text{oc}}$  upon 1 wt % CaCO<sub>3</sub> coating on the TiO<sub>2</sub> surface. The highest power conversion efficiency for the coated cell was as high as 10.2%, as shown in Figure 6, when an antireflective layer (SiO<sub>2</sub>/Al<sub>2</sub>O<sub>3</sub>/ZrO<sub>2</sub>/MgF<sub>2</sub>, Tokai Optical Co., Ltd., Japan) was put on the cell surface.<sup>16</sup>

The increase in  $V_{\text{oc}}$  is associated with the conduction band-edge shift and suppression of charge recombination. Since we did not observe a band-edge shift using the spectroelectrochemistry method (see Figure S2 in Supporting Information), the  $V_{\text{oc}}$  increase should be mainly attributed to suppression of charge recombination. To clarify the coating effect, it is informative to study the electron recombination behavior using IMVS. IMVS, whose details can be found elsewhere,<sup>24</sup> was carried out at open circuit with various light intensities. The DC photocurrent of the measured cell was measured under the same light intensity as that for IMVS measurement. Electron lifetime was extracted from angular frequency ( $\omega_{\text{min}}$ ) in the IMVS plot, where the minimum

(23) Wang, Z.-S.; Hara, K.; Dan-oh, Y.; Kasada, C.; Shinpo, A.; Suga, S.; Arakawa, H.; Sugihara, H. *J. Phys. Chem. B* **2005**, *109*, 3907.

(24) Schlichthörl, G.; Huang, S. Y.; Sprague, J.; Frank, A. J. *J. Phys. Chem. B* **1997**, *101*, 8141.

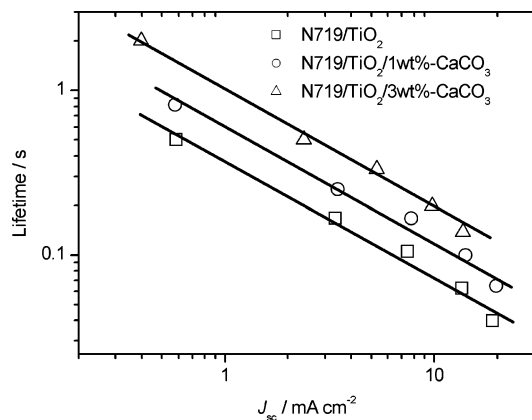


**Figure 7.** Double-logarithmic plot of electron lifetime against short-circuit photocurrent. Illumination: 532 nm laser light with a white light bias; light intensity adjusted with neutral density filters. Two identical samples were measured, and the relative error was below 10%.

imaginary was observed using  $\tau = 1/\omega_{\min}$ .<sup>24,25</sup> Figure 7 shows the relationship between electron lifetime and short-circuit photocurrent. Power-law dependence of electron lifetime on light intensity or electron density was observed for both uncoated and coated cells. Electron lifetime decreased with increasing light intensity. This means that electron recombination with  $I_3^-$  ions becomes faster with increasing light intensity. The electron lifetime was increased by  $\sim 50\%$  upon 1 wt %  $CaCO_3$  coating on the  $TiO_2$  surface and further increased by a factor of 3 upon 3 wt %  $CaCO_3$  coating on the  $TiO_2$  surface. These results indicate that the coated  $CaCO_3$  insulating layer behaves as a barrier to physically separate the injected electrons and oxidized dye cations and  $I_3^-$  ions<sup>8,9,12</sup> and thus increases electron lifetime. The increased

electron lifetime mainly accounts for the increased  $V_{oc}$ . Although the larger coating suppressed charge recombination more efficiently, the significantly decreased  $J_{sc}$  canceled the  $V_{oc}$  enhancement and resulted in a drop of efficiency.

## Conclusions

We demonstrated a simple route to grow an electronic-insulating coating of  $CaCO_3$  on the  $TiO_2$  surface, which increased dye adsorption significantly, resulting in enhanced  $J_{sc}$ , and retarded the charge recombination efficiently, leading to enhanced  $V_{oc}$ . When the amount of  $CaCO_3$  coating was controlled to as small as 1 wt %, both  $J_{sc}$  and  $V_{oc}$  can be improved significantly, resulting in significantly improved power conversion efficiency. However, when a larger amount of coating was applied to the  $TiO_2$  surface,  $V_{oc}$  was further enhanced while  $J_{sc}$  was reduced significantly because the more insulating coating not only blocks electron recombination but also prohibits electron injection, leading to decreased power conversion efficiency. These findings open the way for using an electronic insulating substance as a coating material in DSSCs.

**Acknowledgment.** This work was supported by the New Energy and Industrial Technology Development Organization (NEDO) under the Ministry of Economy Trade and Industry.

**Supporting Information Available:** FT-IR spectra for N719-loaded  $CaCO_3$ -coated and uncoated  $TiO_2$ , and plot of absorbance at 780 nm of  $CaCO_3$ -coated and uncoated  $TiO_2$  as a function of applied potential. This material is available free of charge via the Internet at <http://pubs.acs.org>.

(25) Fisher, A. C.; Peter, L. M.; Ponomarev, E. A.; Walker, A. B.; Wijayantha, K. G. U. *J. Phys. Chem. B* **2000**, *104*, 949.